Two distinct binding sites for globotriaosyl ceramide on verotoxins: identification by molecular modelling and confirmation using deoxy analogues and a new glycolipid receptor for all verotoxins

Per-Georg Nyholm[1], Göran Magnusson[2], Zhiyuan Zheng[2], Raquel Norel[3], Beth Binnington-Boyd[4] and Clifford A Lingwood[4,5]

Background: The *Escherichia coli* verotoxins (VTs) can initiate human vascular disease via the specific recognition of globotriaosyl-ceramide (Gb_3) on target endothelial cells. To explore the structural basis for receptor recognition by different VTs we used molecular modelling based on the crystal structure of VT1, mutational data and binding data for deoxy galabiosyl receptors.

Results: We propose a model for the verotoxin 'cleft-site complex' with Gb_3. Energy minimizations of Gb_3 within the 'cleft site' of verotoxins VT1, VT2, VT2c and VT2e resulted in stable complexes with hydrogen-bonding systems that were in agreement with binding data obtained for mono-deoxy analogues of Gb_3. N-deacetylated globoside (aminoGb$_4$), which was found to be a new, efficient receptor for all verotoxins, can be favorably accommodated in the cleft site of the VTs by formation of a salt bridge between the galactosamine and a cluster of aspartates in the site. The model is further extended to explain the binding of globoside by VT2e. Docking data support the possibility of an additional binding site for Gb_3 on VT1.

Conclusions: The proposed models for the complexes of verotoxins with their globoglycolipid receptors are consistent with receptor analogue binding data and explain previously published mutational studies. The results provide a first approach to the design of specific inhibitors of VT–receptor binding.

Addresses: [1]Department of Molecular and Medical Genetics, University of Toronto, Toronto, Ontario M5S 1A8, Canada, [2]Organic Chemistry, Chemical Center, University of Lund, P.O. Box 124, S-221-00 Lund, Sweden, [3]Department of Computer Science, School of Mathematical Sciences, Tel Aviv University, Tel Aviv 69978, Israel, [4]Department of Microbiology, Research Institute, Hospital for Sick Children, Toronto, Ontario M5G 1X8, Canada and [5]Departments of Clinical Biochemistry, Biochemistry and Microbiology, University of Toronto, Toronto, Ontario, Canada.

Correspondence: Clifford A Lingwood
email: cling@sickkids.on.ca

Key words: Carbohydrate–protein docking, glycolipid conformation, molecular recognition, Shiga-like toxin B subunit

Received: **12 Jan 1996**
Revisions requested: **30 Jan 1996**
Revisions received: **7 Mar 1996**
Accepted: **21 Mar 1996**

Chemistry & Biology April 1996, **3**:263–275

Introduction

Verotoxins (VTs) are *Escherichia coli* subunit toxins comprising a single ~30 kDa A-subunit, which has N-glycanase activity [1] and is responsible for inhibition of protein synthesis, and five noncovalently associated 7.5 kDa receptor-binding B-subunits [2,3]. The family of verotoxins includes VT1, VT2 and VT2c, all of which are implicated in the microvascular pathologies hemorrhagic colitis and hemolytic uremic syndrome (HUS) [4] and bind to globotriaosylceramide (Gb_3: galα1-4galβ1-4glc ceramide). The remaining verotoxin, VT2e (the pig edema disease toxin [5,6]), binds to Gb_3 and globotetraosyl ceramide (Gb_4: galNAcβ1-3galα1-4galβ1-4glc ceramide) [7]. There is a high incidence of HUS in children following gastrointestinal infection with verotoxin-producing *E. coli*; this correlates with the selective expression of Gb_3 in the pediatric renal glomerulus [8]. Thus it is likely that the epidemiology of this disease is determined by receptor distribution [9]. It has been suggested that oral administration of matrix-bound Gb_3 oligosaccharide within the gastrointestinal tract may provide a novel means of reducing the incidence or severity of HUS symptoms by reducing VT translocation into the circulation [10].

Cultured endothelial cells can be verotoxin sensitive [11,12], and their sensitivity can be modulated by cytokines [13–17]. Gb_3 is also a human B-cell differentiation antigen [18,19], involved in signal transduction through the α_2-interferon receptor [20–22] and CD19 [23], both of which contain a VT1 B-subunit-like binding site for Gb_3 [24,25]. B-subunit binding to Gb_3-positive B-lymphocytes results in the induction of apoptosis [26], and verotoxin binding abrogates B-cell function *in vitro* [27]. A similar induction of apoptosis is seen after holotoxin treatment of vero [28] and astrocytoma (S. Arab *et al.*, unpublished data) cells, and the increased Gb_3 synthesis of certain human tumours renders them sensitive to verotoxin killing *in vitro* and *in vivo* ([29], S. Arab *et al.*, unpublished data).

Thus, defining the molecular basis of Gb_3 recognition by the B-subunit pentamer will be important to understand the basis of human vascular disease and B-cell differentiation, and to develop neoplastic therapies. Although

the crystal structure of the verotoxin B-subunit pentamer [30] and holotoxin [31] have been determined, it is probable that solubility problems will prevent the co-crystallization of verotoxin with its receptor glycolipid. The toxin does not bind [32,33], or binds very poorly [34], to the free oligosaccharide moiety from Gb_3 ($K_d \sim 10^{-3}$ M, as compared to $K_d \sim 10^{-9}$ M for Gb_3). We have therefore used a combination of theoretical calculation and experimental binding to glycolipid receptor analogues to predict the precise location of the Gb_3 binding site within the known crystal structure of the VT1 B-subunit. In a preliminary report [35], we proposed a model of the Gb_3–VT1 B-subunit complex in which the galα1-4gal moiety is docked into a crevice close to the interface between adjacent B-subunits (site I or the 'cleft site'). Here we show that N-deacetylated Gb_4 (aminoGb$_4$) is a new, efficient receptor for all VTs that is well accommodated in the cleft site. We extend our model to explain the binding of Gb_3 by the various natural VTs, and the additional binding of Gb_4 by VT2e. We also define a second potential carbohydrate binding site on the verotoxin B-subunit that may be more important in the binding of Gb_3 by the other members of the verotoxin family, particularly VT2c binding to Gb_3 that contains a C18 fatty acid [36].

Results

Binding of aminoGb$_4$

Although Gb_4 is the preferred receptor for VT2e, this glycolipid is not recognized above background by VT1, VT2 or VT2c (Fig. 1). Selective deacetylation of the terminal galNAc residue by basic hydrolysis, as previously described [37], generates a glycolipid that is avidly bound by all members of the verotoxin family (Figs 1,2). By thin-layer chromatography overlay, the binding of VT1 and VT2e to aminoGb$_4$ is approximately equivalent to their binding to Gb_3 and Gb_4, respectively, whereas VT2 and VT2c bind aminoGb$_4$ preferentially (Fig. 1). In the microtitre assay, aminoGb$_4$ is as effective as the preferred receptor for each toxin (Fig. 2). Binding to the N-dimethylated derivative of aminoGb$_4$ was as effective as binding to aminoGb$_4$ (data not shown). Thus, toxin binding was probably facilitated by the deacetylation of Gb_4 because of the generation of charge on the amine, not by the steric effect of the loss of the acetyl group. The charge by itself is insufficient to confer binding, however, since similarly N-deacetylated gangliotriaosyl ceramide [37] was not bound (data not shown).

Modelling of the VT1–aminoGb$_4$ complex

Calculations of electrostatic potentials were performed on the VT1 B-subunits using the DelPhi program to locate favourable binding sites for an NH_3^+ function. A major domain of negative potential is contained within the previously described site I ('cleft site') [35] for binding of the carbohydrate moiety of Gb_3 (see Supplementary material and [35]). This negative potential is mainly due to an Asp triplet (Asp16-Asp17-Asp18) located in a loop at the interface between adjacent subunits. The corresponding DelPhi calculations on aminoGb$_4$ (see Supplementary material) reveals a complementary positive region, comprising the NH_3^+ group and a positively charged patch, extending across the α-galactose to the hydrophobic face of the β-galactose moiety.

Modelling of aminoGb$_4$ in site I based on our previous model of the VT1–Gb_3 complex placed the NH_3^+ group of galactosamine close enough to the Asp triplet to form a salt bridge with the carboxyl of Asp16 (Fig. 3a). This carboxyl group is also the acceptor for a hydrogen bond from the 3-OH group of the galactosamine. In addition, two hydrogen bonds were established between the galactosamine 4-OH group and the amino-terminal Thr1 of the adjacent subunit. The globotriaose portion of aminoGb$_4$ formed seven hydrogen bonds with the protein (Table 1, Fig. 3a,b). These interactions are also present in the proposed model of the VT1 site I–Gb_3 complex (Fig. 3d). The hydrogen bonding system is shown schematically in Figure 3b.

The curvature of the galα1-4gal moiety is sterically complementary to the crevice lined by Phe30, Thr21 and Asn15 in site I. A 90° projection of the complex (Fig. 3c) shows that the galα1-4gal moiety is snugly accommodated. The conformation of aminoGb$_4$ in the complex is almost identical to the minimum energy conformation of unbound aminoGb$_4$ as calculated with GESA and Discover (Table 2; for details see Materials and methods). The conformation

Figure 1

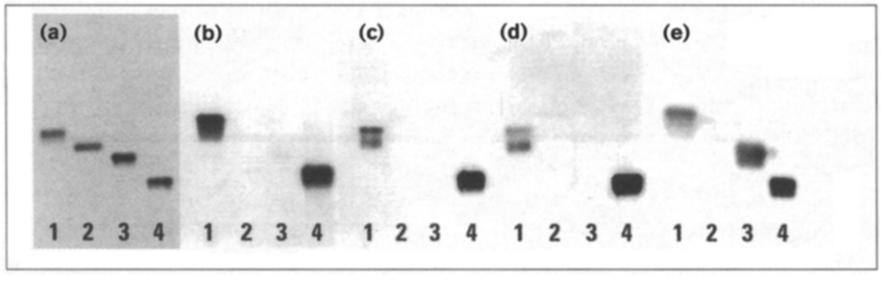

AminoGb$_4$ binds to all members of the verotoxin family. The figure shows a thin-layer chromatography overlay assay of verotoxin binding to glycolipids Gb_3 (lane 1), Gg_3 (galNAcβ1-4galβ1-4glc ceramide; lane 2), Gb_4 (lane 3) and aminoGb$_4$ (lane 4). **(a)** Orcinol detection of all lipids. **(b)** VT1, **(c)** VT2, **(d)** VT2c and **(e)** VT2e binding.

Figure 2

Binding of verotoxins to glycolipids. **(a)** VT1, **(b)** VT2, **(c)** VT2c and **(d)** VT2e were tested for binding to Gb_3 (■), Gb_4 (△) and aminoGb$_4$ (❑) in microtitre plate format.

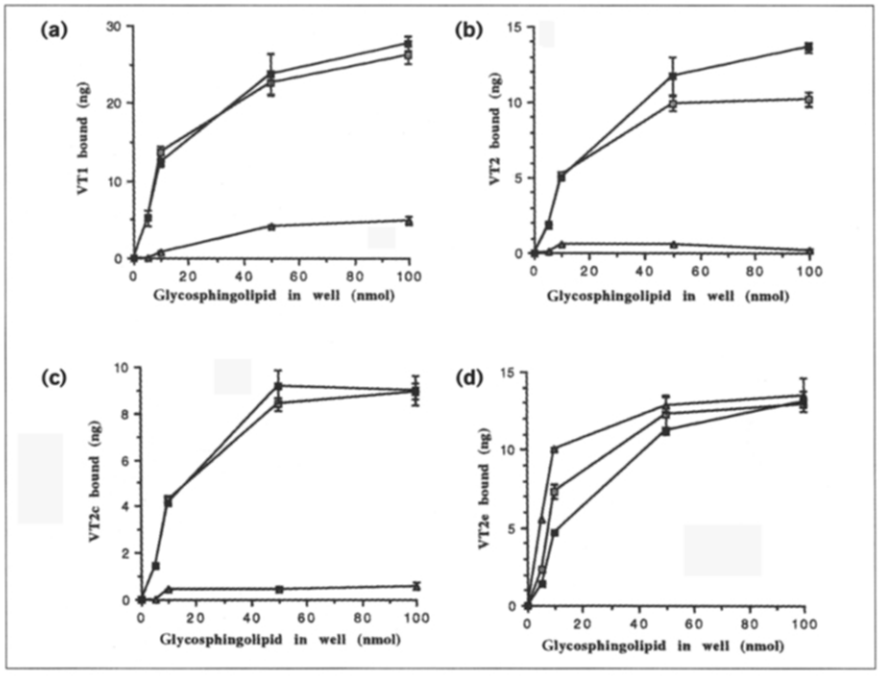

of the glucose-ceramide linkage of aminoGb$_4$ (Fig. 3a) is conformer 2 according to earlier molecular mechanics calculations [38]. This conformation, unlike the other two favoured conformations for the glcβ1-1ceramide linkage (numbers 5 and 6), allows the hydrocarbon chains of the ceramide to extend from the protein with an orientation compatible with packing in a lipid bilayer.

Modelling of cleft site complexes of verotoxins with Gb_3

The docking of Gb_3 in the cleft site of VT1 [35] was further refined with energy minimizations in the presence of a shell of explicit water molecules (Fig. 3d). Similar calculations were performed for the complexes of Gb_3 with VT2 and VT2e (Fig. 4), which had been modelled by homology to the VT1 B-subunit crystal structure. In addition to the hydrogen bonds Thr21OH to galαO6 and galβ6OH to Asp17 in VT1, reported in our preliminary studies [35], the galα6OH is also hydrogen bonded to the side chain of Glu28 (which is reoriented from the crystal coordinates), and galα2OH is hydrogen bonded to Asp17, galα4OH to Lys13 and galβ2OH to Gly60 (Table 1). Corresponding hydrogen bonds were also observed in complexes of VT2, VT2c and VT2e with Gb_3, except that the hydrogen bond at galβ6OH is considerably weakened by the replacement of Asp16 by Asn in VT2c (Table 1).

The axially oriented 4-hydroxyl group of the galα points into a polar pocket lined by the side-chain carbonyl of Asn15, the NH_3^+ group of Lys13 and the carboxyl group of Glu65 of the adjacent B-subunit (Fig. 3d). The galα4OH group is within hydrogen bonding distance of all these three groups, but in VT1 these hydrogen bonds tend to be weak. This is because the carboxyl group of Glu65 has a restricted mobility and is shielded as a hydrogen bond acceptor because of close interactions (a hydrogen bond and ionic contacts) with Lys13 and the amino-terminal Thr1 of the adjacent subunit. For VT2 and VT2c, in which Thr1 is missing, the calculations predict significantly stronger hydrogen bonds for the galα4O group (with Lys 12 and Glu64). In the VT1–Gb_3 complex, the galα3O group is not involved in hydrogen bonding with the protein. The adjacent carboxyl group of Glu65 is not available as an acceptor due to the interaction with Thr1 mentioned above. However, in VT2 and VT2c the galα3OH can establish a strong hydrogen bond with the corresponding carboxyl group of Glu64. In the VT2e–Gb_3 complex, a hydrogen bond in the opposite direction (from the side chain amide nitrogen of Gln64 to galα3O) is predicted.

The glcβ6O was also within hydrogen-bonding distance of the carbonyl oxygen of Gly60 in VT1 and the corresponding Gly59 in the VT2s. This hydrogen bond is weak and donation can either take place to surrounding water (as in the VT1–Gb_3 complex) or to glcβO5. In VT2 and VT2c, the glcβ6OH preferentially establishes a hydrogen bond to the carboxyl group of Glu57.

Two intramolecular hydrogen bonds in the Gb_3 trisaccharide were also observed in all the complexes: glcβ3OH to galβ5O and galβ3OH to galα5O. A hydrogen bond

Figure 3

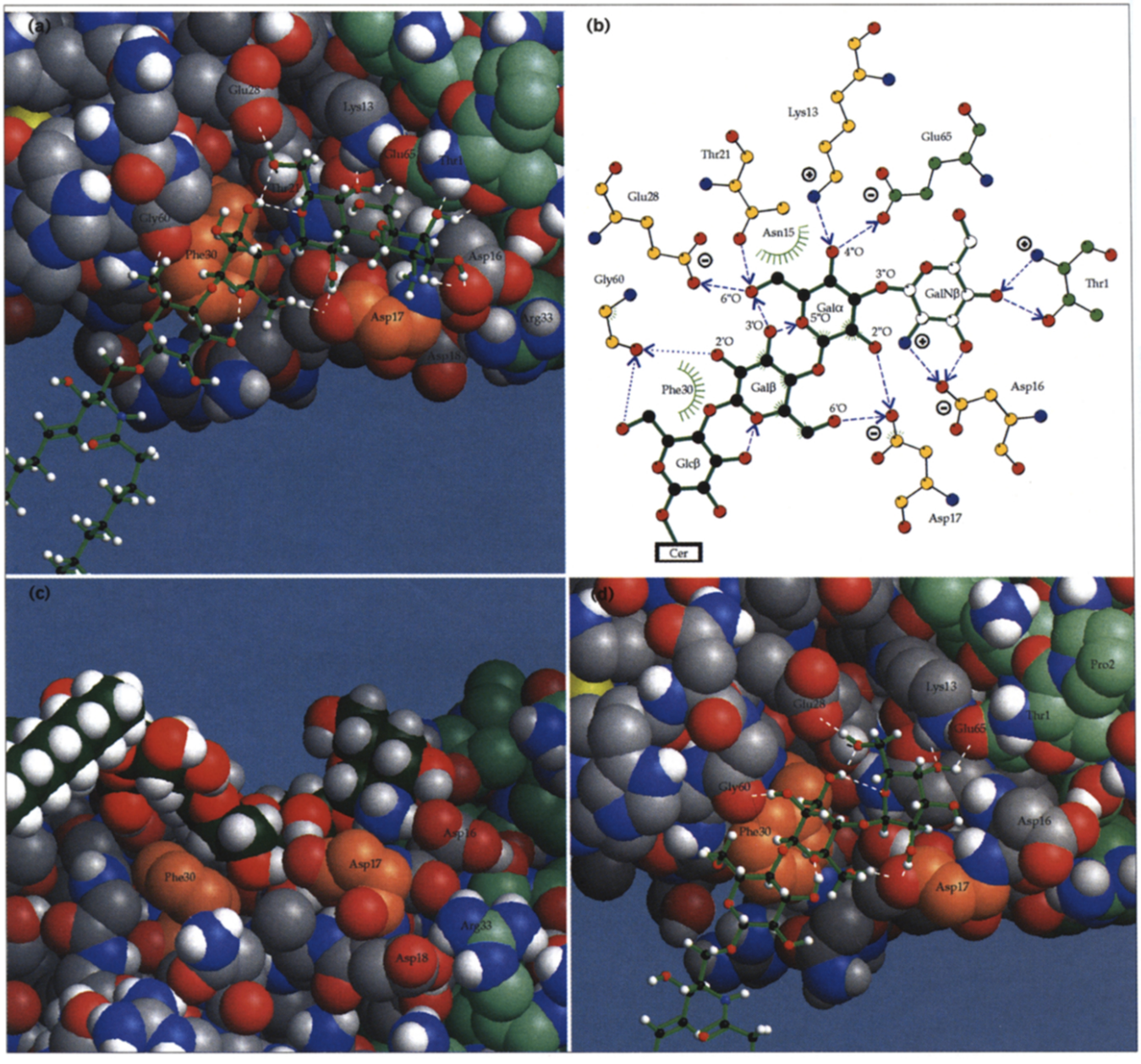

AminoGb$_4$ and Gb$_3$ docked in site I (cleft site) of VT1. **(a)** Side view of aminoGb$_4$ docked in site I. **(b)** Schematic of interactions of aminoGb$_4$ in site I. Dashed arrows indicate the calculated hydrogen bonds of the complex, weak hydrogen bonds are shown as dotted lines and non-polar van der Waals contacts are shown as green spikes. The diagram was created using the Ligplot/HBplus programs [70]. **(c)** The VT1 B-subunit–aminoGb$_4$ complex in (a) rotated 90° to show the membrane-facing surface of the toxin. The salt bridge in the complex from the galNH$_3^+$ to Asp16 reorients the Asp16 side chain leading to the loss of the Asp16–Arg33 salt bridge, present in the crystal structure of the VT1 B-subunit pentamer. **(d)** Side view of Gb$_3$ docked in site I. In (a), (c) and (d) the protein is shown with space-filling atoms, as is the glycolipid in (c). A ball and stick representation is used for the glycolipid in (a) and (d). Carbon atoms of the fourth B-subunit (left) are shown in black; those of the third subunit are in green. The carbons of Phe30 and Asp17 are orange. Non-polar hydrogens in the protein have been omitted. Hydrogen bonds are indicated with dashed white lines. The subunit surface which faces the target cell membrane is directed down. For an overview of the receptor binding sites see the supplementary material and [35].

between galβ3OH and galα6O was formed in all the complexes except VT2e–Gb$_3$ and VT2e–Gb$_4$. Table 1 lists the hydrogen bonds for all site I complexes studied, with the calculated donor–acceptor distances.

There is extensive hydrophobic contact between the hydrophobic face of the galβ and the side chain of Phe30 in the complexes of VT1 with Gb$_3$ and aminoGb$_4$ (Fig. 3). In the case of the VT2 complexes (Figs 4, 5), a similar hydrophobic

Table 1

Hydrogen bonds in the minimized verotoxin-glycolipid complexes.

Complex		VT1–aminoGb$_4$	VT1–Gb$_3$	VT2,VT2c–Gb$_3$	VT2e–Gb$_3$	VT2e–Gb$_4$
Donor	Acceptor	Donor–acceptor distance (Å)	Donor–acceptor distance (Å)	Donor–acceptor distance (Å)	Donor–acceptor distance (Å)	Donor–acceptor distance (Å)
Gln64 HE1	galNAc4O	na	na	na	na	3.1
Gln64 HE2	galNAc5O	na	na	na	na	2.8
galNβ 2NH	Asp16 OD2	2.8[a]	na	na	na	na
galNβ 3OH	Asp16 OD2	2.9	na	na	na	na
Thr1NH	galN 4O	2.8	na	na	na	na
galNβ4O	Thr1 OH	2.8	na	na	na	na
galα 2OH	Asp16[b] (Glu15*) OD2	2.9	2.9	2.8[c]	2.9	2.9
galα 3OH	Glu65(64*) OE1	na	–	2.8	na	na
galα 4OH	Glu65(64*) OE1	2.8[d]	2.7[d]	[e]	na	na
Gln64 HE2	galα 3O	na	na	na	2.9	–
Gln64 HE2	galα 4O	na	na	na	3.2	3.3
Lys13(12*) NZH	galα 4O	2.9[d]	2.8[d]	2.8	2.8	2.7
Lys13(12*) NZH	galα 6O	–	–	–	2.7	
Thr21(20*) OH	galα 6O	2.8	2.8	2.8	2.9	2.8
galα 6OH	Glu28(27*)OE2	2.7	2.7	2.7	2.9	2.9
galβ 2OH	Gly60(59*)O	–	2.9	3.0	3.0	2.9
galβ 6OH	Asp16 (Glu15*) OD2	2.8	2.6	2.7[c]	2.7	2.6
Trp29 NE1H	galβ 6O	na	na	2.9[d]	[e]	[e]
glcβ 6OH	Gly60(59*) O	2.73	[e]	[e]	2.8	2.9
glcβ 6OH	Glu57 OE1	na	na	2.7	na	na
Intra-saccharide bonds						
galβ 3OH	galα 6O	2.8	2.8	2.8	–	–
galβ 3OH	galα 5O	3.1	3.1	2.4	2.9	2.9
glcβ 3OH	galβ 5O	3.0	2.7	2.8	2.7	3.0
galNAc 3OH	galNAc 7O	na	na	na	na	2.7

[a]Superimposed H-bond/salt bridge.
[b]VT1 numbering used. Asterisk refers to equivalent amino acid in VT2's.
[c]Missing in VT2c.
[d]Weak H-bond due to suboptimal angle geometry.
[e]Observed in minimizations and/or MD without explicit water.
na, not applicable

surface is provided by Trp29. Although this side chain is larger in size, the indole is less able to align efficiently with the galβ, probably due to the fact that the bulkier indole is more restricted by surrounding side chains of the protein.

Modelling of the VT2e–Gb$_4$ complex

Energy minimizations of Gb$_4$ within the cleft site of VT2e (Fig. 5) showed that the terminal galNAcβ residue can be favourably accommodated in contact with Glu15 and the side chain of Gln64 of the adjacent subunit. A strong hydrogen bond is seen between the side-chain amide nitrogen of Gln64 and the 4O of the galNAc. Furthermore, the acetamido group of the galNAc establishes van der Waals contacts in a shallow trough between the side chains of Asp16 and Glu15. The hydrogen bond interactions of the α- and β-galactoses are maintained as compared to the VT2e–Gb$_3$ complex (Table 1). The ϕ/ψ torsional angles of the glycosidic linkages of Gb$_4$ in the complex with VT2e are listed in Table 2. For the globotriaose moiety, the agreement with the other complexes is <±10°, while the galNAcβ1-3galα linkage shows a moderate (25°) deviation from the ϕ/ψ values of the VT1–aminoGb4 complex and the corresponding unbound tetrasaccharide. The ϕ/ψ angles for the galNAcβ1-3galα linkage in the VT2e–Gb$_4$ complex are still within a favourable range, however, since this linkage characteristically has a shallow potential-energy well [39].

Binding studies with deoxy Gb$_3$ analogues

In parallel with the modelling studies we assayed the binding of verotoxins to monodeoxy Gb$_3$ analogues in which specific hydroxyl groups of the terminal and penultimate galactose residues have been removed. Binding was monitored both by thin-layer chromatography

Table 2

Calculated minimum energy conformations of the saccharide moieties of the glycolipid receptors Gb$_3$, aminoGb$_4$ and Gb$_4$ in the unbound state and complexed (at site I) with verotoxins.

		Glycosidic linkages (ϕ/ψ)[a]		
Molecules	Program	galN(Ac)β1-3galα	galα1-4galβ	galβ1-4glcβ
Gb$_3$ free	HSEA[b]		−39°/−14°	58°/0°
Gb$_3$–VT1	AMBER[c]		−48°/−4°	55°/−5°
Gb$_3$–VT2	AMBER[c]		−41°/−1°	33°/−17°
Gb$_3$–VT2e	AMBER[c]		−30°/−3°	46°/−10°
aminoGb$_4$ free	HSEA[b]	56°/1°	−39°/−14°	57°/−10°
aminoGb$_4$ free	AMBER[c]	62°/−19°	−36°/−6°	55°/−6°
aminoGb$_4$–VT1	AMBER[c]	49°/−3°	−37°/−5°	40°/10°
Gb$_4$ free	AMBER[c]	58°/−12°	−35°/2°	60°/1°
Gb$_4$–VT2e	AMBER[c]	35°/−29°	−28°/1°	48°/4°

[a]The ϕ/ψ torsion angles are defined as ϕ = H1-C1-O1-Cx, ψ = C1-O1-Cx-Hx. For a complete list and interaction energies see the supplementary material.
[b]HSEA calculation using GESA.
[c]Amber-potentials using the Discover program (ε = 1 with explicit water).

Figure 4

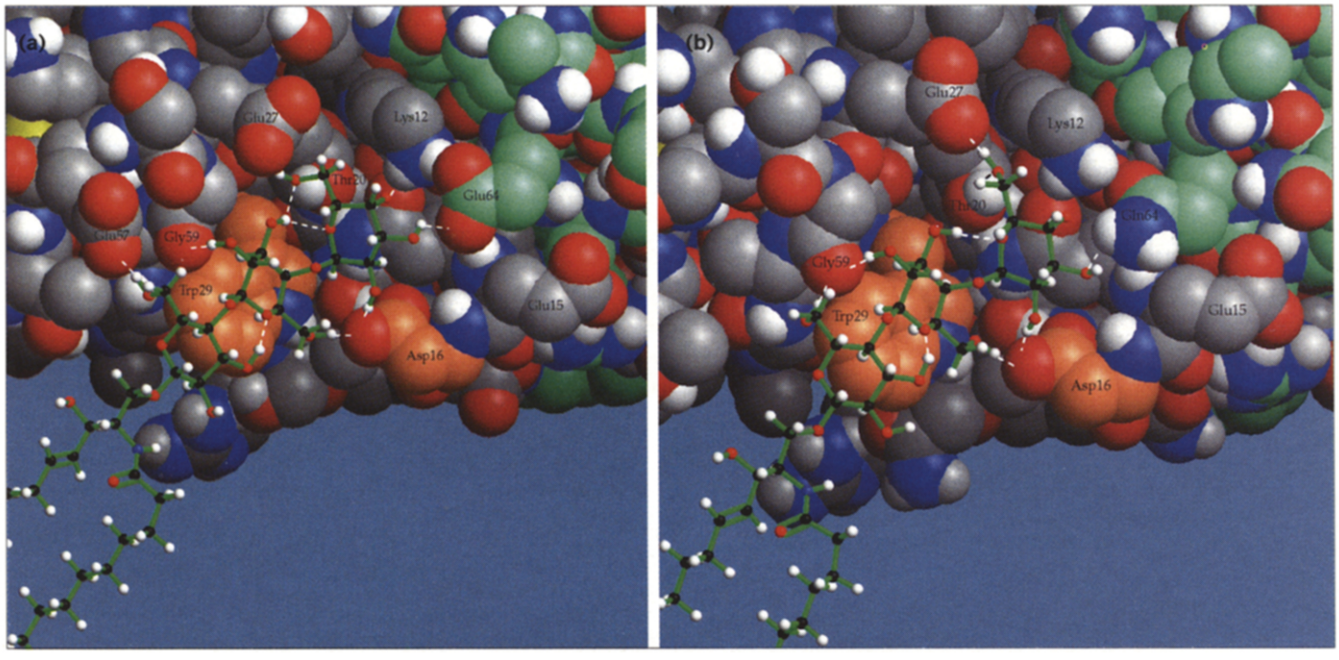

Gb_3 docked into site I of **(a)** VT2 and **(b)** VT2e. In the VT2–Gb_3 complex, the α-galactose makes a strong H-bond through O3 with the carboxyl group of Glu64 in the adjacent subunit. In the case of VT2e–Gb_3, Gln64 donates an H-bond to galα3O. The representation is as for Figure 3a.

overlay for VT1 (Fig. 6) and binding within a phospholipid matrix in microtitre wells (Fig. 7) for all VTs. Although VT1 binding to the parent synthetic analogue as assayed by thin-layer chromatography overlay is considerably less than for natural Gb_3, as we have previously noted [33], we were still able to observe the effect of deoxysugar substitution. The hydroxyl requirement for VT1 was in reasonable agreement with that determined by receptor binding in the microtitre phospholipid matrix which was used for quantitative assessment. All hydroxyls within the galabiose are required for full binding. The reduction in binding following individual hydroxyl deletions was: for VT1, 6" and 6' > 2' > 4" > 2" > 3' and 3" > Gb_3; for VT2, 6", 6', 4" and 3" > 2' > 2" > 3' > Gb_3; for VT2c, 6" and 4" > 2' and 3" > 2" and 6' >> 3' > Gb_3; and for VT2e, 6", 6' and 3" > 3' and 2' > 2" > 4" > Gb_3.

The patterns of binding of VT1, VT2, VT2c and VT2e to these deoxy Gb_3 analogues are clearly distinguishable (Fig. 7). The primary differences are: the more significant role of the 4"OH in VT2 and VT2c binding, the requirement of the 3"OH for the binding of VT2s (particularly VT2e) but not VT1, the greater significance of the 3'OH for VT2e binding and the relative lack of effect of 6'OH removal on VT2c binding.

Docking in site II

The Gb_3 oligosaccharide can also be favourably docked into site II [35] of VT1 (Fig. 8) using an automatic program [40,41] which detects complementarity in shape between receptor and ligand. Several possible docking positions were identified in site II, but only a few permit suitable orientation of the ceramide for inclusion in a membrane bilayer, considering the favoured conformations of the glcβ1→1ceramide linkage [42]. Of these few, the one with the best van der Waals contacts was subjected to energy minimization. Several hydrogen bonds that involve the galabiose moiety (Ser64NH→galα6O, galα6OH→Lys53, galα3OH→Asp16 and galβ2OH→Asn32) were found after minimization of this complex. As shown in Figure 8, this orientation of the saccharide in site II is compatible with bilayer packing of the ceramide moiety when adopting conformer 6 for the glcβ1→1ceramide linkage.

Discussion

AminoGb$_4$ binding and docking model

We have identified a new glycolipid receptor for verotoxins *in vitro*, which is at least as active as any receptor species previously described for any member of the verotoxin family. By thin-layer chromatography overlay, aminoGb$_4$ is the preferred receptor for all verotoxins (Fig. 1). Although the physiological relevance of this binding has yet to be established, toxin recognition of aminoGb$_4$ *in vitro* provides an important insight into the structural basis of the specificity of the different verotoxins for different receptors. We have previously speculated that there are two potential Gb_3-binding sites per B-subunit monomer [35]. The present studies show that, whereas it has not been possible to accommodate

Figure 5

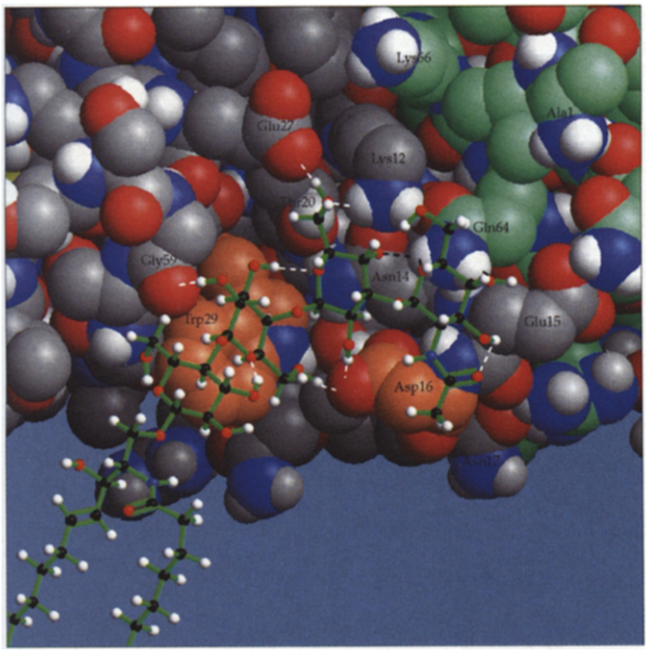

Gb_4 docked into site I of VT2e. Note that the galNAcβ is in proximity to the side chain of Gln64 of the adjacent B subunit. The NAc group is accommodated in a trough between Asp16 and Glu15. A hydrogen bond between the galNAcβ3OH and the oxygen of the NAc group is indicated by a dashed line.

aminoGb$_4$ in the second site irrespective of the conformation of the saccharide–ceramide linkage, it can be effectively docked in site I, the 'cleft' site (Fig 3a). This can be explained by the formation of a salt bridge between the NH_3^+ group of aminoGb$_4$ and the carboxyl group of Asp16 and additional electrostatic interactions with the carboxyl groups of Asp17 and Asp18 that, together with Asp16, generate a focus of negative potential in this region of site I (see Supplementary material). The charge of the amino group and the partial positive charges across the α- and β-galactoses, provide a continuous positive surface on the face of the terminal trisaccharide that is next to the toxin to complement the negative charge within the cleft site (see Supplementary material). Preliminary studies indicate that complexes of aminoGb$_4$ with site I of the other verotoxins are stabilized by similar electrostatic interactions.

As shown in Table 2, only minor conformational changes of the ϕ/ψ angles, as compared to the minimum energy conformation in the free state, are required to fit the saccharide moiety of aminoGb$_4$ into site I of VT1. The galα1-4galβ linkage, which is known to be the most restricted of the three glycosidic linkages, only has to undergo changes of a few degrees. The required changes in ϕ/ψ values for the galβ1–4glcβ and the galNβ1-3galα linkages are < 20°. This can be achieved without significant energy penalties, since both of these types of linkages, particularly the latter, have considerable flexibility [39].

The fact that N-dimethylated aminoGb$_4$ is efficiently bound indicates that additional methyl groups can be accommodated without perturbing the structure of the complex. This is consistent with a model in which the amino function of the galactosamine is located at the surface of the Asp16–Asp18 loop, allowing interaction with a more bulky positively charged group. The inability of VT1 to bind Gb$_4$ is probably a result of electrostatic repulsion between the carbonyl oxygen of the NAc group (missing in aminoGb$_4$) and the carboxyl group of Asp16.

Deoxy sugar analogue binding: confirmation of the cleft site (site I) model

The data on the binding of the deoxy Gb$_3$ analogues to all the verotoxins (Fig. 7) are in excellent agreement with

Figure 6

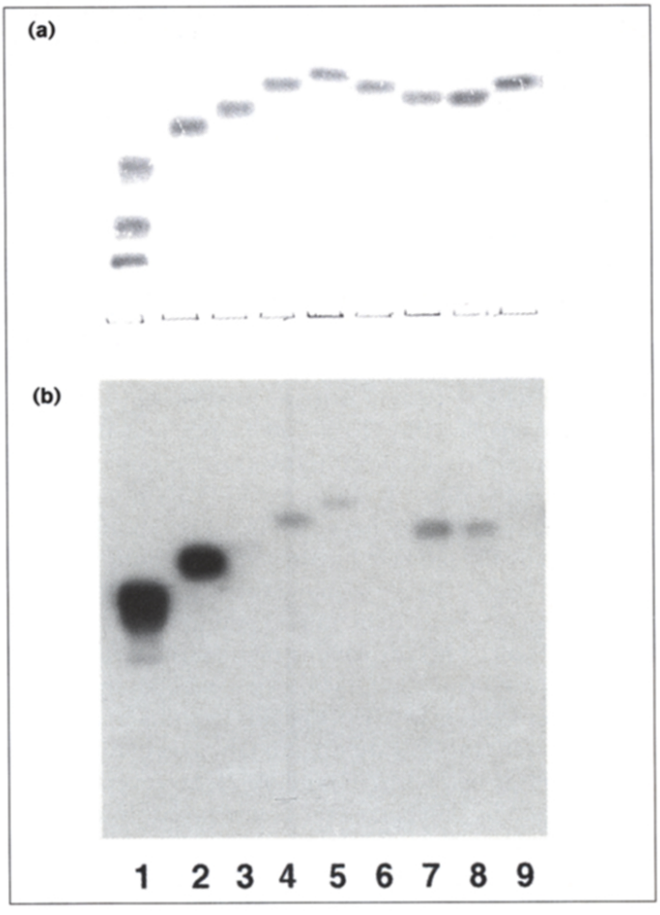

^{125}I-VT1 binding to deoxy Gb$_3$ bisalkyl analogues. **(a)** Orcinol detection of glycolipids by thin-layer chromatography overlay. **(b)** VT1 binding. Lanes 1) Gb$_3$, Gb$_4$ and Forssman, 2) parent Gb$_3$ bisalkyl analogue, 3) 2" deoxy, 4) 3" deoxy, 5) 4" deoxy, 6) 6" deoxy, 7) 2' deoxy, 8) 3'deoxy, and 9) 6' deoxy analogues. Sample size was 2 μg for each glycolipid.

Figure 7

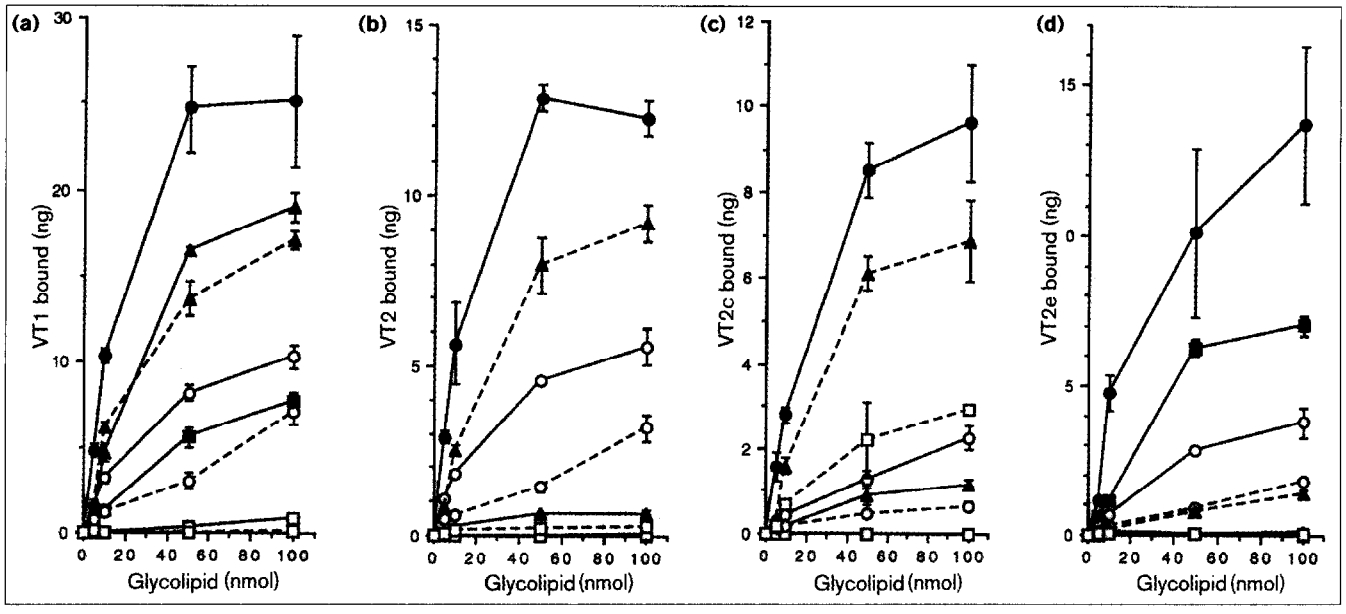

Microtitre binding assay of deoxyGb_3 analogues by ^{125}I-labelled-verotoxins. **(a)** VT1, **(b)** VT2, **(c)** VT2c and **(d)** VT2e were assayed for binding to Gb_3 (control: ●), 2" deoxy Gb_3 (○), 3" deoxy Gb_3 (▲), 4" deoxy Gb_3 (■), 6" deoxy Gb_3 (□), 2' deoxy Gb_3 (--○--), 3' deoxy Gb_3 (--▲--) and 6' deoxy Gb_3 (--□--). Data for deoxy analogues of the β-galactose are shown as dotted lines. In comparison to the parent unmodified species, percentage binding of VT1, VT2, VT2c or VT2e to the deoxy analogues were: for galα6 deoxy Gb_3 3 %, <1 %, <1 %, <1 %; for galα4 deoxy Gb_3 31 %, <1 %, <1 %, 51 %; for galα3 deoxy Gb_3 76 %, 5 %, 12 %, <1 %; for galα2 deoxy Gb_3 41 %, 45 %, 23 %, 28 %; for galβ6 deoxy Gb_3 <1 %, 2 %, 30 %, <1 %; for galβ3 deoxy Gb_3 68 %, 75 %, 71 %, 10 %; for galβ2 deoxy Gb_3 28 %, 26 %, 7 %, 13 %. (Ratios were determined in the presence of 100 nmole of glycolipid).

hydrogen bond predictions from the docking computations. Previous studies of monodeoxygalabioses indicate that the overall conformation of the disaccharide is not altered by such modification [43]. The requirement for the 6"OH is consistent with the prediction that it forms hydrogen bonds with Thr21 and Glu28, and the 6'OH requirement for VT1, VT2 and VT2e binding is consistent with a hydrogen bond to Asp17 (VT1 numbering). The 4"OH requirement for VT2 and VT2c binding can be explained by the predicted hydrogen bond to the carboxyl group of Glu64. In VT1, however, the corresponding residue, Glu65, is partially buried and interacts with the amino-terminal Thr1, explaining the reduced requirement for the galα4O (Fig. 7). Glu65 is beyond hydrogen-bond distance of galα3O in VT1 (Fig. 3d) and this hydroxyl is less important for VT1 binding to Gb_3 as opposed to the other toxins (Fig. 7). In VT2 and VT2c, however, the lack of restriction by Thr1 and Pro2 would probably allow the exposed carboxyl group of the corresponding residue, Glu64, to hydrogen bond with galα3O and galα4O, thus explaining the selective requirement for these hydroxyls for receptor binding by these toxins (Fig. 7). In the VT2e–Gb_3 complex these carboxyl hydrogen bonds are lost due to the substitution Glu64→Gln, but a hydrogen bond in the opposite direction, from the side chain amide nitrogen to galα3O, is formed. This would explain the requirement for the galα3OH for VT2e binding (Fig. 7).

In the minimized complexes, the galβ3OH forms intramolecular hydrogen bonds with O5 (and O6) of galα,

Figure 8

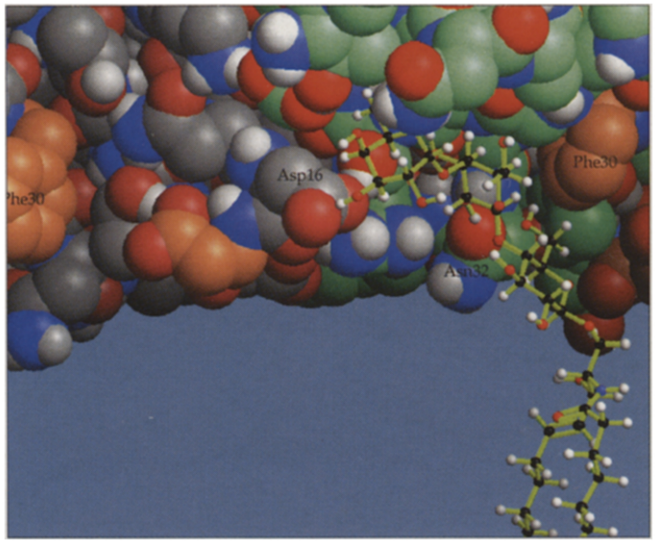

Gb_3 conformer 6 docked in site II of VT1. The terminal α-galactose forms the following hydrogen bonds with the toxin: Ser64NH→galα6O, galα6OH→Lys53O, galα3OH→Asp16. Only one hydrogen bond to the β-galactose (galβ2OH→Asn32OD1) is observed.

rather than interacting with the protein (Table 1). An intramolecular hydrogen bond between galβ3OH and galα5O has also been observed in the crystal structure of galabiose [44]. The intrasaccharide hydrogen bonds are likely to stabilize the conformation of the galα1-4galβ linkage and thus favour interactions of the galabiose moiety with the protein. This may explain the reduction in binding seen for the 3'deoxy analogue (Fig. 7).

Comparison of Gb_3 docking in site I of VT1, 2, 2c and 2e

The modelling of the site I complexes indicates that Asp17 is a crucial hydrogen bond acceptor for galβ6OH and galα2OH. This is important, since the corresponding residue in VT2c (which is of ~1000 fold lower cytotoxicity and has a reduced Gb_3 binding affinity as compared to VT1 [45,46]) is asparagine (Asn16). Mutation of this Asn in VT2c to Asp results in a dramatic increase in cytotoxicity [47], probably because the affinity of Gb_3 binding increases due to formation of a hydrogen bond between galβ6OH and the carboxyl group of Asp16. Consistent with this model, the 6' deoxy sugar substitution had markedly less effect on the binding of VT2c than of VT1, VT2 or VT2e (Fig. 7). It is also possible that the substitution Asp16→Asn in VT2c allows closer proximity to the π-system of Trp29, restricting cleft site access.

The amino acid residues forming site I in the verotoxins are highly conserved within the verotoxin family. This region of conservation was noted in the original crystallographic studies and was therefore suggested as a potential receptor-binding site [30]. Moreover, the sequence forming site I in the verotoxins shows extensive similarity with CD19, which binds globo-series carbohydrates (globotriaose and globotetraose) [23]. The α_2-interferon receptor also shows amino acid similarity with VT site I and binds globo-series glycosphingolipids [22]. The existence of these sequence similarities among proteins which all recognize glycolipids of the globo series is in agreement with the proposed role of site I as a binding site for galα1-4gal-containing saccharides.

Comparison of the model with mutational analyses

Glu65 in VT1 has been mutated to Gln [48], resulting in complete loss of receptor recognition. This observation is consistent with our modelling, which indicates a galα4O ›Glu65 hydrogen bond and predicts the loss of this hydrogen bond on substitution with Gln in VT1 (data not shown). Mutation of the equivalent residue in VT2e (Gln64→Glu) [49] was involved in the alteration of binding specificity from $Gb_4 + Gb_3$ to Gb_3 alone. Mutation of Phe30→Ala results in a loss of Gb_3 binding [50], consistent with the alignment of the hydrophobic side of the β-galactose with the phenyl ring in the cleft site. Mutation of Gly59 in VT2 (or Gly60 in VT1) has been shown to result in >50 % loss of receptor binding [51], which would be consistent with involvement of this residue in site I (see Table 1). Loss of Gb_3 binding after mutation of Arg33 [51] is more consistent with binding at site II, although Arg33 is involved in a salt bridge to Asp16 [31] in site I of VT1 (Fig. 3c). Loss of receptor binding following removal of the carboxy-terminal four amino acids in VT2 [52] is also consistent with site I usage. Furthermore, the loss of Gb_3 binding following the double mutation Asp16→His, Asp17→His in VT1 [48] and the increased potency of VT2c after mutation of Asn16→Asp [47] are consistent with the proposed involvement of Asp16 and Asp17 in site I.

Model for recognition of Gb_4 by VT2e: crucial role of Gln64

VT2e is the only toxin that binds Gb_4, while all the VTs bind Gb_3 and aminoGb_4 (Fig. 1). Several amino acid substitutions in VT2e within the cleft binding site, as described above, explain this difference in binding specificity. In VT1, the pocket between the side chains of Asp16 and Asp17 is not sufficient to accommodate the acetamido group of Gb_4. In particular, the close approach of the oxygen of the NAc group towards the carboxyl group of Asp16 would disfavour Gb_4 interaction with VT1. This explanation is consistent with the observation that mutation of Asp18 to Asn in VT1 allows Gb_4 binding [49]. In this mutant, the mutual electrostatic repulsion within the Asp16–Asp18 loop is reduced, allowing the carboxyl group of Asp16 to reorient and thus avoid interference with the acetamido group. The side chain of Gln64 in VT2e also has a capacity to hydrogen bond with the carboxyl group of Glu15, thus stabilizing a trough between the side chains of Glu15 and Asp16 that accommodates the NAc group of Gb_4 (Fig. 6).

In the modelled complexes of VT2 and VT2c with Gb_3, the 3"OH group donates a strong hydrogen bond to the carboxyl group of Glu64. In the case of Gb_4, the 3"OH is blocked by the galNAc substitution and cannot act as an H-donor to Glu64. The O1 and O5 atoms of the added galNAc would instead cause steric and electrostatic repulsion with the carboxyl group of Glu64. This is a likely explanation for the lack of Gb_4 binding by VT2 and VT2c. In VT2e, however, Glu64 is replaced by a glutamine residue, which stabilizes the VT2e–Gb_4 complex by donating a hydrogen bond to the galNAc4O and potentially also to the O1 and O5 oxygens of this moiety. This model of the VT2e–Gb4 complex is consistent with the fact that GT3, a double mutant of VT2e (Gln64→Glu, Lys66→Gln) [49], does not bind Gb_4, though Gb_3 binding is retained. Neither mutation alone affected Gb_4 binding. The lack of effect of the single mutation Lys66→Gln is consistent with the model since residue 66 makes no direct contact with the Gb_4 saccharide bound in the cleft site. The fact that the single mutation Gln64→Glu in VT2e does not block binding of galNAc (by interactions similar to those discussed for VT2 and VT2c) can be explained by the attraction of the Glu64

side chain to the adjacent positive region formed by Lys66, Lys12 and the amino terminus (Ala1). In the double mutant GT3, the substitution Lys66→Gln decreases this attraction and thus increases the propensity of the side chain of Glu64 to extend and interfere with Gb_4 binding. Validation of this interpretation must await the availability of quantitative binding data and crystal structures of VT2e and its mutants.

Most of the interactions which stabilize the VT2e–Gb4 complex are contained within a single B-subunit monomer. Only about 10 % of the interaction energy is due to the adjacent B-subunit. Residues in the carboxyl terminus of the adjacent B-subunit do, however, prevent the binding of Gb_4 by VT2 and VT2c. Therefore, we would predict that if monomeric VT2 B-subunits (VT2, 2c or 2e) were produced, these would also bind Gb_4. This possibility is further supported by the finding that CD19, which has an amino-terminal extracellular domain that shows sequence similarity to the VT B-subunit [23], does not contain residues equivalent to the extramonomeric sequences involved in verotoxin site I–Gb_3 binding [24] and binds both globotriaose and globotetraose oligosaccharides [23].

Receptor binding in site II

Previous calculations with the GRID program indicated a favourable second binding site (site II) for the Gb_3 oligosaccharide in the region of Gly62, Asn32 and Phe30 [35], but a different glycolipid conformer (number 6 [38]) was required as compared to site I. It was speculated that site II might function in Gb_3 binding by VT2c and VT2, which show a preference for Gb_3 containing C18 fatty acids, while VT1 prefers Gb_3 with longer fatty acid chains [36,53]. If the fatty acid chain length affects the glycolipid conformation, the resultant binding in different sites would explain the relative lack of inhibition of VT1 binding by VT2c and *vice versa* [36].

The present studies, using an automatic docking program, confirm that Gb_3 conformer 6 can be accommodated in site II (Fig. 8). Several fits were found; the most favourable is shown in Figure 8. In this position, the galα3O is oriented towards the side chain of Asp16. Modelling indicates that an additional galNβ or galNAcβ residue linked to the 3-position of the α-galactose of Gb_3 in site II would essentially extend away from the protein surface, devoid of favourable contacts with the toxin. In contrast, the site I complexes calculated for VT1–aminoGb$_4$ and VT2e–Gb_4 allow a number of favourable interactions for the terminal amino sugar with the protein. We thus conclude that aminoGb$_4$ and Gb_4 are very likely to bind only in site I.

The significance of Gb_3 binding in site II of VT2c or any other verotoxin cannot be inferred from our present study. Since our site II model is not in agreement with the binding data for deoxy analogues of Gb_3, and none of the synthetic analogues studied preferentially bind VT2c, it is likely that the VT2 and VT2c binding presently observed is restricted to the cleft site, as for VT1. Our calculations indicate that the interaction energy of the site II VT1–Gb_3 complex is only 50 % of that calculated for site I. Moreover, the model of binding at site II cannot readily explain the importance of Phe30 (in VT1) and Asp16 (in VT2) for Gb_3 binding suggested by mutational studies [47,50].

It is of interest, however, to note that the modelling suggests that Gb_3 binding in site II would not interfere with Gb_3 binding in site I. It may thus be speculated that, due to the effects of multivalency, even partial occupancy of site II would increase the overall affinity of the interaction. The recognition of different conformers by the two sites might ensure efficient receptor recognition in a variety of cell membranes with different lipid compositions. Further studies are required to establish the relative significance of site I and site II in different verotoxins. These studies might also shed light on a series of poorly understood factors affecting the affinity of verotoxin–Gb_3 interactions, such as fatty-acid chain length of the receptor [36,53,54] and the matrix lipids [55], receptor concentration in the bilayer [33] and the method of immobilization of the receptor glycolipid [33,55]. An understanding of these phenomena, which apparently relate to the steric presentation of the saccharide epitope [56], is important for the design of high affinity inhibitors of VT–Gb_3 interactions.

Preliminary X-ray analysis of a cocrystal of VT1 B-subunits with globotriaose oligosaccharide (R. Read, personal communication) indicate density primarily in the region of site II and in the region of Trp34. Density due to saccharide was later also resolved in the region of site I (Ling, H., Boodhoo, A., Armstrong, G.D., Brunton, J.L. & Read, R.J., poster W127, Proceedings of the American Crystallographic Association Annual Meeting, Montréal, Quebec, Canada, July 1995). Although these data are only in partial agreement with our modelling, they do support the proposal of two binding sites (sites I and II). It is possible that cocrystallization with the oligosaccharide does not reproduce the steric presentation that applies when the saccharide is presented on the surface of a lipid bilayer, and is coupled to a lipid moiety anchored within the bilayer. Thus it is our contention that molecular modelling combined with detailed binding studies is currently the preferred method for localization of the glycolipid binding site in this system.

Significance

The binding of verotoxin to globotriaosyl ceramide on human endothelial cells is the basis for the vascular pathology of hemorrhagic colitis and hemolytic uremic syndrome (HUS). HUS results in significant pediatric mortality and long term renal insufficiency. The model

we present here for verotoxin–Gb_3 interactions provides a framework for the rational design of novel high affinity soluble inhibitors with therapeutic potential.

The verotoxin–Gb_3 interaction is an intriguing example of protein–carbohydrate recognition. Although verotoxins are galabiose-binding ligands, high affinity interactions only occur in the context of glycolipid structures. Since glycolipids and proteins cannot be easily co-crystallized or studied by NMR due to solubility problems, molecular modelling is an important tool for the study of this receptor–ligand interaction.

We have precisely defined a region at the cleft between adjacent B-subunits as the major Gb_3 binding site. Our binding model predicts the high binding affinity of aminoGb$_4$, a new, preferred receptor glycolipid for all verotoxins, and explains how amino-acid differences found in the carboxyl terminus of VT2e allow Gb_4 binding. Different hydroxyl group requirements in the galabiose moiety are demonstrated for the binding of each verotoxin and the molecular basis of these requirements are explained by our model.

The model also explains the importance of the lipid moiety in VT–Gb_3 binding, as only one of the possible conformations of the sugar-lipid linkage allows efficient binding in the proposed 'cleft site'. We also propose a second binding site, which accommodates a different conformer. This site may be significant for VT2c binding, thus explaining the lack of competition between VT1 and VT2c for receptor binding [36]. This suggests that under appropriate conditions the B-subunit pentamer could have a maximum receptor valency of ten, potentially doubling the receptor's binding capacity.

Materials and methods

The neutral glycolipid fraction from human renal tissue was prepared as described previously [57]. Gb_3 and Gb_4 were separated by silica-gel chromatography. Verotoxin-unreactive Gb_4 was deacetylated by aqueous base hydrolysis to give a ceramide tetrasaccharide containing a free terminal galactosamine residue (aminoGb$_4$) [37]. VT1 was purified from pJLB28 [58], VT2 from R94 [59], VT2c from E3211 [45] and VT2e from pGT100 [49]. VT2 and VT2c were purified by Gb_3 affinity chromatography [60]. Affinity purification had no effect on glycolipid-receptor binding specificity.

Deoxy Gb_3 analogues

Deoxy derivatives of the terminal and penultimate sugars of a synthetic Gb_3 analogue containing globotriaose in anomeric linkage to a bis-C16-alkyl sulfone aglycone (compound B5 in Boyd *et al.* [33]) were synthesized as described [61,62]. The deoxy compounds were standardized by benzoylation-HPLC analysis [57] and the glycosphingolipids were standardized using a sphingosine assay [63].

Verotoxin–glycolipid binding

The thin-layer chromatography overlay assay of ^{125}I-VT [46,64] binding was performed as described [65,66]. Quantitative analysis of receptor function in a phospholipid matrix was carried out in microtitre plates using a modification of our previously described procedure [33,36]. Plates were coated with 50 µl of methanol containing 50 ng phosphatidyl choline, 25 ng cholesterol and 0, 5, 10, or 100 ng receptor glycolipid and allowed to dry overnight at room temperature. Before binding, plates were blocked with 0.5 % BSA in phosphate buffered saline (PBS) for 1 h at room temperature and washed three times with PBS. ^{125}I-labelled toxin was added to wells in triplicate (100 ng per well in 100 µl PBS containing 0.5 % BSA) and incubated for 1 h at room temperature. After extensive washing, the wells were cut out and bound radioactivity counted.

Modelling

All the calculations of VT1 binding were performed using the coordinates from the crystal structure of the pentamer of B-subunits of VT1 [30]. The B-subunits of VT2, VT2c and VT2e were homology modelled starting from VT1 B. The oligomer binding (OB) fold motif present in VT1 has been observed in a number of oligosaccharide/oligonucleotide binding proteins (see [67] for review). Comparative studies [67] have shown that the barrel–helix frameworks of these structures are superimposable with root-mean square deviations of 1.4–2.2 Å, although the amino-acid sequences are totally unrelated. This indicates that the OB fold in the verotoxins is quite stable and we thus did not expect any significant folding differences between VT1 and the VT2s, which all have a sequence homology of 62–65 % with VT1. In particular, strands 1–3, which are involved in site I, only show conservative substitutions when comparing VT2, VT2c and VT2e with VT1. For these reasons the procedure for modelling the VT2s was limited to side chain substitution followed by energy minimizations (Insight II/Discover with AMBER parameters). This was done for a system of two adjacent B-subunits (numbers three and four) initially with fixed backbone and subsequently with restraints for the backbone.

The minimum energy conformations of the saccharide moieties of Gb_3, aminoGb$_4$ and Gb_4, respectively, were obtained with the GESA program [38]. For the proximal glcβ1-1ceramide linkage and the lipid moiety, favoured conformations were adopted from previous studies with molecular mechanics (MM3) [38]. Electrostatic surface properties of VT1 and of aminoGb4 were analyzed using the DelPhi program [68].

Energy minimizations for the different complexes (VT1–Gb_3, VT2–Gb_3, VT2c–Gb_3, VT2e–Gb_3, VT1–aminoGb$_4$ and VT2e–Gb_4) were performed on systems consisting of a dimer of B-subunits (numbers three and four) and the saccharide moiety of the respective glycolipid. The calculations were carried out with the Discover program (Biosym Inc.) using the AMBER all-atom parameter set and saccharide parameters developed by Homans [69]. The starting orientation of the galα1-4galβ moiety in site I was obtained from previous calculations [35]. The minimizations were initially performed with a distance-dependent dielectric constant ($\epsilon = 4r$) with a fixed peptide backbone. For each system several minimizations were carried out with somewhat different starting orientations for the saccharide and different conformations for the side chains of Glu28 (VT1 numbering) and Gln64 (VT2e). Short molecular dynamics (MD) simulations (10–15 ps) followed by minimizations were also performed. The energetically most favourable geometry found in these MM and MD runs was subject to energy minimization (steepest descent and conjugate gradient) with a 5 Å shell of explicit water molecules (at $\epsilon = 1$). The restraints for the protein were gradually released, maintaining only light tethering for the peptide backbone in the final stage. The minimizations were continued until the maximum derivative was < 0.001 kcal Å^{-1}.

To locate additional possible binding sites on the B-subunit, an automatic docking procedure that detects shape complementarity [40,41] was applied. Using this method, the Gb_3 and aminoGb$_4$ saccharides were docked with a dimer of B-subunits (numbers three and four) of VT1. Elimination of orientations with unfavourable van der Waals clashes was performed in the presence of the adjacent two subunits (numbers two and five). Typically about 500 orientations were obtained. These were manually inspected and assessed in terms of

compatibility with the lipid packing of the ceramide, considering the three preferred conformers for the ceramide–saccharide linkage [42].

Molecular manipulation and display for production of pictures were performed with the ChemX program (Chemical Design Ltd, Oxford).

Acknowledgements

This work was supported by MRC program grant no. PG 11123 (to C.A.L.), the Mizutani Foundation (P.G.N.), the Swedish Medical Research Council (fellowship to P.G.N.), the Swedish Natural Science Research Council (G.M.) and an Eshkol Fellowship (to R.N.). The authors thank Dr M. Mylvaganum for preparation of N-methyl aminoGb$_4$ and valuable discussions, Dr I. Pascher for a critique of the manuscript and M. Lundmark, MEDNET, for assistance with colour printing.

Supplementary material

Includes an overview figure summarizing the two sites of verotoxin binding, an electrostatic potential map for VT site I and aminoGb$_4$, and expanded versions of Tables 1 and 2 with detailed geometric and interaction energies.

References

1. Endo, Y., *et al.*, & Igarashi, K. (1988). Site of the action of a vero toxin (VT2) from *Escherichia coli* O157:H7 and a Shiga toxin on eukaryotic ribosomes. *Eur. J. Biochem.* **171**, 45–50.
2. Ramotar, K., *et al.*, & Brunton, J. (1990). Characterization of Shiga-like toxin 1 B subunit purified from overproducing clones of the SLT-1 B cistron. *Biochem. J.* **272**, 805–811.
3. Lingwood, C.A. (1993). Verotoxins and their glycolipid receptors. In *Advances in Lipid Research.* (Bell, R., Hannun, Y.A. & Merrill Jr, A. eds), pp. 189–212, Academic Press, San Diego.
4. Karmali, M.A. (1989). Infection by verocytotoxin-producing *Escherichia coli. Clin. Microbiol. Rev.* **2**, 15–38.
5. Linggood, M.A. & Thompson, J.M. (1987). Verotoxin production among porcine strains of *Escherichia coli* and its association with edema disease. *J. Med. Microbiol.* **24**, 359–362.
6. MacLeod, D.L., Gyles, C.L. & Wilcock, B.P. (1991). Reproduction of edema disease of swine with purified Shiga-like toxin-II variant. *Vet. Pathol.* **28**, 66–73.
7. DeGrandis, S., Law, H., Brunton, J., Gyles, C. & Lingwood, C.A. (1989). Globotetraosyl ceramide is recognized by the pig edema disease toxin. *J. Biol. Chem.* **264**, 12520–12525.
8. Lingwood, C.A. (1994). Verotoxin binding in human renal sections. *Nephron* **66**, 21–28.
9. Taylor, C.M. (1995). Verocytotoxin-producing *Escherichia coli* and the haemolytic uraemic syndrome. *J. Infect.* **30**, 189–192.
10. Armstrong, G.D., Fodor, E. & Vanmaele, R. (1991). Investigation of Shiga-like toxin binding to chemically synthesized oligosaccharide sequences. *J. Infect. Dis.* **164**, 1160–1167.
11. Obrig, T.G., *et al.*, & Rothman, S.W. (1988). Direct cytotoxic action of Shiga toxin on human vascular endothelial cells. *Infect. Immun.* **56**, 2373–2378.
12. Obrig, T., *et al.*, & Daniel, T. (1993). Endothelial heterogeneity in Shiga toxin receptors and responses. *J. Biol. Chem.* **268**, 15484–15488.
13. Louise, C.B. & Obrig, T.G. (1992). Shiga toxin-associated hemolytic uremic syndrome: combined cytotoxic effects of Shiga toxin and lipopolysaccharide (endotoxin) on human vascular endothelial cells *in vitro. Infect. Immun.* **60**, 1536–1543.
14. Louise, C.B. & Obrig, T.G. (1991). Shiga toxin-associated hemolytic uremic syndrome: combined cytotoxic effects of Shiga toxin, interleukin-1β, and tumor necrosis factor alpha on human vascular endothelial cells *in vitro. Infect. Immun.* **59**, 4173–4179.
15. Kaye, S.A., Louise, C.B., Boyd, B., Lingwood, C.A. & Obrig, T.G. (1993). Shiga toxin-associated hemolytic uremic syndrome: interleukin-1β enhancement of Shiga toxin cytotoxicity toward human vascular endothelial cells *in vitro. Infect. Immun.* **61**, 3886–3891.
16. van der Kar, N.C.A.J., Monnens, L.A.H., Karmali, M. & van Hinsbergh, V.W.M. (1992). Tumor necrosis factor and interleukin-1 induce expression of the verotoxin receptor globotriaosyl ceramide on human endothelial cells: implications for the pathogenesis of the hemolytic uremic syndrome. *Blood* **80**, 2755–2764.
17. van der Kar, N.C.J., *et al.*, & van Hinsbergh, V.W.M. (1995). Tumor necrosis factor α induces endothelial galactosyl transferase activity and verocytotoxin receptors. Role of specific tumor necrosis factor receptors and protein kinase C. *Blood* **85**, 734–743.
18. Mangeney, M., Richard, Y., Coulaud, D., Tursz, T. & Wiels, J. (1991). CD77: an antigen of germinal center B cells entering apoptosis. *Eur. J. Immunol.* **21**, 1131–1140.
19. Gregory, C.D., *et al.*, & Lipinski, M. (1987). Identification of a subset of normal B cells with a Burkitt's lymphoma (BL)-like phenotype. *J. Immunol.* **139**, 313–318.
20. Cohen, A., Hannigan, G.E., Williams, B.R.G. & Lingwood, C.A. (1987). Roles of globotriosyl- and galabiosylceramide in verotoxin binding and high affinity interferon receptor. *J. Biol. Chem.* **262**, 17088–17099.
21. Lingwood, C.A. & Yiu, S.C.K. (1992). Glycolipid modification of α-interferon binding: sequence similarity between α-interferon receptor and the verotoxin (Shiga-like toxin) B-subunit. *Biochem. J.* **283**, 25–26.
22. Ghislain, J., Lingwood, C.A. & Fish, E.N. (1994). Evidence for glycosphingolipid modification of the type 1 IFN receptor. *J. Immunol.* **153**, 3655–3663.
23. Maloney, M.D. & Lingwood, C.A. (1994). CD19 has a potential CD77 (globotriaosyl ceramide)-binding site with sequence similarity to verotoxin B-subunits: Implications of molecular mimicry for B cell adhesion and enterohemorrhagic *Escherichia coli* pathogenesis. *J. Exp. Med.* **180**, 191–201.
24. Lingwood, C.A. (1996). Role of verotoxin receptors in pathogenesis. *Trends Microbiol.* **4**, 147–153.
25. Lingwood, C.A. (1996). Aglycone modulation of glycolipid receptor function. *Glycoconjugate J.*, in press.
26. Mangeney, M., *et al.*, & Wiels, J. (1993). Apoptosis induced in Burkitt's lymphoma cells via Gb$_3$/CD77, a glycolipid antigen. *Cancer Res.* **53**, 5314–5319.
27. Cohen, A., *et al.*, & Dosch, H.-M. (1990). Expression of glycolipid receptors to Shiga-like toxin on human B lymphocytes: a mechanism for the failure of long-lived antibody response to dysenteric disease. *Int. Immunol.* **2**, 1–8.
28. Inward, C.D., *et al.*, & Taylor, C.M. (1995). Verocytotoxin-1 induces apoptosis in vero cells. *J. Infect.* **30**, 213–218.
29. Farkas-Himsley, H., Hill, R., Rosen, B., Arab, S. & Lingwood, C.A. (1995). The bacterial colicin active against tumour cells *in vitro* and *in vivo* is verotoxin 1. *Proc. Natl. Acad. Sci. USA* **92**, 6996–7000.
30. Stein, P.E., Boodhoo, A., Tyrrell, G.J., Brunton, J.L. & Read, R.J. (1992). Crystal structure of the cell-binding B oligomer of verotoxin-1 from *E. coli. Nature* **355**, 748–750.
31. Fraser, M., Chernaia, M., Kozlov, Y. & James, M. (1994). Crystal structure of the holotoxin from *Shigella dysenteriae* at 2.5 Å resolution. *Nat. Struct. Biol.* **1**, 59–64.
32. Lindberg, A.A., *et al.*, & Karlsson, K.-A. (1987). Identification of the carbohydrate receptor for Shiga toxin produced by *Shigella dysenteriae* type 1. *J. Biol. Chem.* **262**, 1779–1785.
33. Boyd, B., Zhiuyan, Z., Magnusson, G. & Lingwood, C.A. (1994). Lipid modulation of glycolipid receptor function: availibility of Galα1-4Gal disaccharide for verotoxin binding in natural and synthetic glycolipids. *Eur. J. Biochem.* **223**, 873–878.
34. St. Hilaire, P.M., Boyd, M.K. & Toone, E.J. (1994). Interaction of the Shiga-like toxin type 1 B-subunit with its carbohydrate receptor. *Biochemistry* **33**, 14452–14463.
35. Nyholm, P.-G., Brunton, J.L. & Lingwood, C.A. (1995). Modelling of the interaction of verotoxin-1 (VT1) with its glycolipid receptor, globotriaosylceramide (Gb$_3$). *Int. J. Biol. Macromol.* **17**, 199–205.
36. Kiarash, A., Boyd, B. & Lingwood, C.A. (1994). Glycosphingolipid receptor function is modified by fatty acid content: verotoxin 1 and verotoxin 2c preferentially recognize different globotriaosyl ceramide fatty acid homologues. *J. Biol. Chem.* **269**, 11138–11146.
37. Lingwood, C.A. and Nutikka, A. (1994). A novel chemical procedure for the selective removal of nonreducing terminal N-acetyl residues from glycolipids. *Anal. Biochem.* **217**, 119–123.
38. Nyholm, P.-G. & Pascher, I. (1993). Steric presentation and recognition of the saccharide chains of glycolipids at the cell surface: favoured conformations of the saccharide–lipid linkage calculated using molecular mechanics (MM3). *Int. J. Biol. Macromol.* **15**, 43–51.
39. Gronberg, G., Nilsson, U., Bock, K. & Magnusson, G. (1994). Nuclear magnetic resonance and conformational investigations of the pentasaccharide of the Forssman antigen and overlapping di-, tri-, and tetra-saccharide sequences. *Carbohydr. Res.* **257**, 35–54.
40. Norel, R., Lin, S.L., Wolfson, H.J. & Nussinov, R. (1994). Shape complementarity at protein–protein interfaces. *Biopolymers* **34**, 933–940.
41. Norel, R., Lin, S.L., Wolfson, H.J. & Nussinov, R. (1995). Molecular surface complementarity at protein–protein interfaces; the critical role played by surface normals at well placed, sparse points in docking. *J. Mol. Biol.* **252**, 263–273.

42. Nyholm, P.-G. & Pascher, I. (1993). Orientation of the saccharide chains of glycolipids at the membrane surface: conformational analysis of the glucose-ceramide and the glucose-glyceride linkages using molecular mechanics (MM3). *Biochemistry* **32**, 1225–1234.
43. Bock, K., Frejd, T., Kihlberg, J. & Magnusson, G. (1988). Synthetic receptor analogues: the conformation of methyl 4-O-α-D-galacto-pyranosyl-β-D-galactopyranoside (methyl β-D-galabioside) and related derivatives, determined by NMR and computational methods. *Carbohydr. Res.* **176**, 253–270.
44. Svensson, G., Albertsson, J., Svensson, C., Magnusson, G. & Dahmen, J. (1986). X-ray crystal structure of galabiose, O-alpha D-galactopyranose-(1-4)-D-galactopyranose. *Carbohydr. Res.* **146**, 29–38.
45. Head, S.C., Petric, M., Richardson, S.E., Roscoe, M.E. & Karmali, M. (1988). Purification and characterization of verocytotoxin 2. *FEMS Microbiol. Lett.* **51**, 211–216.
46. Head, S., Karmali, M. & Lingwood, C.A. (1991). Preparation of VT1 and VT2 hybrid toxins from their purified dissociated subunits: Evidence for B subunit modulation of A subunit function. *J. Biol. Chem.* **266**, 3617–3621.
47. Lindgren, S.W., Samuel, J.E., Schmitt, C.K. & O'Brien, A.D. (1994). The specific activities of Shiga-like toxin type II (SLT-II) and SLT-II-related toxins of enterohemorrhagic *Escherichia coli* differ when measured by Vero cell cytotoxicity but not by mouse lethality. *Infect. Immun.* **62**, 623–631.
48. Jackson, M.P., Wadolkowski, E.A., Weinstein, D.L., Holmes, R.K. & O'Brien, A.D. (1990). Functional analysis of the Shiga toxin and Shiga-like toxin type II variant binding subunits by using site-directed mutagenesis. *J. Bacteriol.* **172**, 653–658.
49. Tyrrell, G.J., *et al.*, & Brunton, J.L. (1992). Alteration of the carbohydrate binding specificity of verotoxins from Galα1-4Gal to GalNAcβ1-3Galα1-4Gal and vice versa by site-directed mutagenesis of the binding subunit. *Proc. Natl. Acad. Sci. USA.* **89**, 524–528.
50. Clark, C., *et al.*, & Brunton, J. (1996). Phenylalanine 30 plays an important role in receptor binding of verotoxin-1. *Mol. Microbiol.* **19**, 891–899.
51. Perera, L.P., Samuel, J.E., Holmes, R.K. & O'Brien, A.D. (1991). Identification of three amino acid residues in the B-subunit of Shiga toxin and Shiga-like toxin type II that are essential for holotoxin activity. *J. Bacteriol.* **173**, 1151–1160.
52. Perera, L.P., Samuel, J.E., Holmes, R.K. & O'Brien, A.D. (1991). Mapping the minimal contiguous gene segment that encodes functionally active Shiga-like toxin II. *Infect. Immun.* **59**, 829–835.
53. Kiarash, A., Boyd, B. & Lingwood, C.A. (1994). The role of the lipid moiety in glycolipid receptor function. Model studies of verotoxin binding to fatty acid homologues of globotriaosylceramide demonstrate lipid-dependent alterations in carbohydrate receptor function. In *Recent Advances in Verocytotoxin Producing* E. coli *Infections.* (Karmali, M.A. & Goglio, A.G. eds), pp. 175–187, Elsevier Science, B.V., Bergamo, Italy.
54. Pellizzari, A., Pang, H. & Lingwood, C.A. (1992). Binding of verocytotoxin 1 to its receptor is influenced by differences in receptor fatty acid content. *Biochemistry* **31**, 1363–1370.
55. Arab, S. & Lingwood, C.A. (1996). Influence of phospholipid chain length on verotoxin/Gb_3 binding in model membranes: comparison of a surface bilayer film and liposomes. *Glycoconjugate J.*, in press.
56. Strömberg, N., Nyholm, P.-G., Pascher, I. & Normark, S. (1991). Saccharide orientation at the cell surface affects glycolipid receptor function. *Proc. Natl. Acad. Sci. USA* **88**, 9340–9344.
57. Boyd, B. & Lingwood, C.A. (1989). Verotoxin receptor glycolipid in human renal tissue. *Nephron* **51**, 207–210.
58. DeGrandis, S.A., *et al.*, & Brunton, J. (1987). Nucleotide sequence and promoter mapping of the *Escherichia coli* Shiga-like toxin operation of bacteriophage H-19B. *J. Bacteriol.* **169**, 4313–4319.
59. Samuel, J.E., *et al.*, & Krivan, H.C. (1990). Comparison of the glycolipid receptor specificities of Shiga-like toxin type II and Shiga-like toxin type II variants. *Infect. Immun.* **58**, 611–618.
60. Boulanger, J., Huesca, M., Arab, S. & Lingwood, C.A. (1994). Universal method for the facile production of glycolipid/lipid matrices for the affinity purification of binding ligands. *Anal. Biochem.* **217**, 1–6.
61. Zhiyuan, Z. & Magnusson, G. (1994). Synthesis of double-chain bis-sulfone neoglycolipids of the 2''-, 3''-, 4''- and 6''-deoxyglobotrioses. *Carbohydr. Res.* **262**, 79–101.
62. Zhang, Z. & Magnusson, G. (1995). Synthesis of double-chain neoglycolipids of the 2'-, 3'''- and 6''-deoxyglobotrioses. *J. Org. Chem.* **60**, 7304–7315.
63. Naoi, M., Lee, Y.C. & Roseman, S. (1974). Rapid and sensitive determination of sphingosine bases and sphingolipids with fluorescamine. *Anal. Biochem.* **58**, 571–577.
64. Boyd, B., *et al.*, & Lingwood, C. (1993). Alteration of the glycolipid binding specificity of the pig edema toxin from globotetraosyl to globotriaosyl ceramide alters *in vivo* tissue targeting and results in a VT1-like disease in pigs. *J. Exp. Med.* **177**, 1745–1753.
65. Lingwood, C.A., *et al.*, & Karmali, M. (1987). Glycolipid binding of purified and recombinant *Escherichia coli*-produced verotoxin *in vitro*. *J. Biol. Chem.* **262**, 8834–8839.
66. Waddell, T., Head, S., Petric, M., Cohen, A. & Lingwood, C.A. (1988). Globotriosyl ceramide is specifically recognized by the *E. coli* verocytotoxin 2. *Biochem. Biophys. Res. Commun.* **152**, 674–679.
67. Murzin, A.G. (1993). OB (oligonucleotide/oligosaccharide binding)-fold: common structural and functional solution for non-homologous sequences. *EMBO J.* **12**, 861–867.
68. Gilson, M. & Honig, B. (1987). Calculation of electrostatic potentials in an enzyme active site. *Nature* **330**, 84–86.
69. Homans, S.W. (1990). A molecular mechanical force field for the conformational analysis of oligosaccharides: comparison of theoretical and crystal structures of Manα1-3Manβ1-4GlcNAc. *Biochemistry* **29**, 9110–9118.
70. Wallace, A., Laskowski, R. & Thornton, J. (1995). Ligplot – a program to generate schematic diagrams of protein–ligand interactions. *Protein Eng.* **8**, 127–134.